

THE DEGRADATION OF METHYLENE BLUE BY MICROCUBES CATALYST α -Fe₂O₃ VIA HETEROGENOUS FENTON PROCESS

Ngo Thi My Binh, Dinh Van Tac, Doan Van Duong, Trinh Ngoc Dat, Le Vu Truong Son, Vu Thi Duyen*, Vo Thang Nguyen*

The University of Danang - University of Science and Education

*Corresponding author: vtduyen@ued.udn.vn; vtnguyen@ued.udn.vn

(Received: October 19, 2021; Accepted: December 15, 2021)

Abstract - Cubic Fe₂O₃ was synthesized in a facile approach by annealing molecular organic framework Prussian Blue (PB) at 350°C, 550°C, and 650°C. The final product was characterized by IR, Raman and XRD spectroscopic methods illustrating the presence of pure α -Fe₂O₃. SEM images of this material revealed a homogeneous morphology of microcube Fe₂O₃ with a size of about 500 nm. The catalytic activity of cubic Fe₂O₃ was investigated on the degradation of methylene blue in a heterogeneous Fenton system. It was shown that the thermally oxidative decomposition of PB at 550°C has resulted in porous Fe₂O₃ which exhibited highest MB degradation efficiency. In the presence of 0.5 M H₂O₂ and 0.3 g/L Fe₂O₃ at pH = 3.59, 50 ppm MB in studied solution has been removed at a rate constant of 0.0398 min⁻¹, which is comparable with other analogous catalytic materials.

Key words - Cubic α -Fe₂O₃; porous; molecular organic framework; heterogenous Fenton; methylene blue

1. Introduction

Methylene blue (MB) (3,7-bis(Dimethylamino)-phenothiazin-5-iumchloride) (Figure 1) is a thiazine cationic dye commonly found in discharge water of many process industries such as pharmaceutical, textile, leather, cosmetics and paint ones [1]. The environmental risk of organic dyes – containing wastewater is obvious when the stable dyes do not undergo instant degradation under normal condition. Although MB injection is also used to treat methemoglobinemia and urinary tract infections, a long-term exposure to MB, can cause adverse health problems such as difficulties in breathing, vomiting, eye burns, diarrhea and nausea [2-3].



Figure 1. Molecular structure of methylene blue

Fenton reaction is among the most successful approaches to degrade stable organic dyes in wastewater to smaller inorganic compounds. It is well-known that hydroxyl radicals are the key reactive moiety that can oxidize almost all organic compounds in a non-selective way. Conventional Fenton method based on the use of Fe²⁺ solution as the homogeneous catalyst has shown some disadvantages such as the instability of Fe²⁺ solution, the formation of iron sludge which is difficult to separate and recover and also cause secondary pollution. The replacement of homogeneous Fe²⁺ catalyst by solid

catalysts with catalytic active components in heterogeneous Fenton process has overcome the difficulties of the classical method. This method prevents the leaching of iron ion and significantly reduces the formation of iron sludge [4-5]. Also, solid Fenton catalysts are stable and easy to separate, therefore can be recycled for many treatment cycles. However, the most challenge in design such heterogeneous catalyst is the low efficiency and stability as the nano catalyst tends to agglomerate leading to a reduce of catalyst surface area. Therefore, a development of catalyst with both high efficiency and stability is one of the major issues today [6].

Recently, Fe₂O₃ (mainly including α -Fe₂O₃ and γ -Fe₂O₃) and their composites have been extensively studied for wastewater treatment because of their advantages such as chemical abundance, low processing cost and large specific surface area. Especially, it is well-known that Fe₂O₃ nanomaterials exhibit good separation efficiency and cyclic performance on account of their superior magnetic properties. Therefore, the use of Fe₂O₃ material as a heterogeneous catalyst in Fenton process might offer an alternative yet efficient approach for the removal of organic dyes in wastewater [7].

It was shown that the morphology of catalyst material has an important impact on the effectiveness of the Fenton process. Carefully controlling the morphology of Fe₂O₃ during the synthesis process can be beneficial to its use as a heterogeneous catalyst. The molecular organic framework (MOF) has been recently used as a mould in the synthesis of catalytic material with a design morphology, preventing the formation of random catalyst structure, which in turn can improve its catalytic activity. Recently, cubic Fe₂O₃ has been investigated and exhibited high capability in adsorption of various organic pollutants and heavy metal ions [8]. This kind of framework was also used in the synthesis of SnO₂-encapsulated α -Fe₂O₃ nanocubes to be applied as a photo-Fenton catalyst to degrade Rhodamine B [9]. In this paper, the catalytic activity in a Fenton system of pristine cubic Fe₂O₃ prepared from Prussian blue molecular organic framework precursor is presented. This synthesis pathway has resulted in consistent cubic structure of Fe₂O₃ with high surface area which can boost the degradation of MB. The influence of operational parameters was also investigated showing the importance of catalyst dosage, H₂O₂ concentration, solution pH and initial concentration of dye in the removal of MB.

2. Experimental

2.1. Material

Polyvinylpyrrolidone (PVP, K-30, MW ~ 40,000) and $K_4Fe(CN)_6 \cdot 3H_2O$ (Macklin, China); HCl, NaOH, H_2O_2 , methylene blue, methanol (Xilong, China) were purchased and used directly without any further purification. All solutions were prepared using double distilled water.

2.2. Synthesis of Fe_2O_3 microcubes

Prussian Blue microcubes were prepared according to the previous report [8]. The typical procedures were as: 76 g of PVP and 2.2 g of $K_4Fe(CN)_6 \cdot 3H_2O$ added into 1000 mL of 0.1 M HCl under vigorous stirring for 30 minutes until a transparent pale yellow solution was formed. Subsequently, the mixture was placed into an electric oven at 80°C for 24 h. The resulting blue product was centrifuged and rinsed several times with deionized water and ethanol. Afterwards, the as-synthesized PB product was vacuum-dried at 60°C overnight. To obtain the Fe_2O_3 microcubes, the PB sample was transferred to a furnace, heated to 350, 550 and 650°C at a heating rate of 2°C/min and maintained for 6 h. The final products were denoted as Fe_2O_3 -350, Fe_2O_3 -550, Fe_2O_3 -650.

2.3. Material characterization

The obtained sample was characterized by using various chemical and physical techniques. The FT-IR spectra of P- Fe_2O_3 before and after dye's degradation were collected using a JASCO FT/IR-6800 spectrometer (JASCO Analytical Instruments, USA), equipped with a MIRacle™ Single Reflection (ZnSe crystal plate; PIKE Technologies, USA) at room temperature over the range from 4000 to 500 cm^{-1} . The XRD patterns were recorded on a Bruker D8-Advance X-ray powder diffractometer using Cu $K\alpha$ radiation ($\lambda = 1.5406 \text{ \AA}$) with scattering angles (2θ) of 5–70°. Raman spectrum was obtained with Xplora Plus microscope, (Horiba, USA) at excitation laser of 532 nm. The morphology of the sample was observed with the scanning electron microscopy (JEOL JSM-IT200, Japan) with acceleration voltage of 10 kV at a magnification level of 10 K. The surface area of the obtained materials was determined at 77 K by BET analysis using an ASAP 2020 surface area analyzer.

2.4. Heterogeneous Fenton degradation of MB

In a typical test, the Fe_2O_3 catalyst (20–100 mg) was dispersed in 200 mL of a solution containing MB (30 - 100 mg/L) with the assistance of ultrasonic irradiation. The After 30 min of adsorption, H_2O_2 (0.1 – 0.9 M) was added to the reaction system with continuous stirring at room temperature. Mixture was left in the dark to obtain an adsorption equilibrium between MB and the catalyst. The pH of the solution was adjusted by using HCl and NaOH 0.1 M. At desired time intervals, 0.5 mL of samples were collected and diluted to 5.0 mL before filtering through a 0.45 mm nylon syringe filter (FilterBio).

UV–Vis spectroscopy was performed to measure the MB concentration (wavelength of 665 nm). The degradation efficiency of the material was calculated as:

$$H = \frac{C_0 - C}{C_0} \cdot 100\%$$

Where, C_0 and C represent the concentration after adsorption equilibrium and final concentration of MB (mg/L).

The UV-Vis spectra of the studied solutions were recorded using UV-Vis spectrometer Perkin Elmer Lambda 365

The kinetics of photocatalytic degradation of MB in aqueous solution was investigated by the pseudo-first-order model, with the kinetics parameters described as followed:

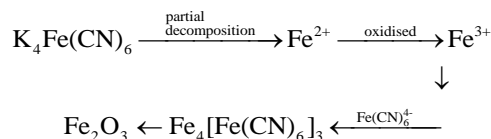
$$\ln \frac{C_0}{C} = kt$$

Where, k (min^{-1}) is the reaction rate constant; and t is the reaction time.

3. Result and discussion

3.1. Characterization of Fe_2O_3 microcubes

The formation of microcubes PB is the result of the decomposition and oxidation of $K_4Fe(CN)_6$ in acidic condition with the addition of PVP as summarized in Scheme 1, in which PVP was used as a surfactant to stabilize the PB particles during the crystallization [10].



Scheme 1. Synthesis pathway of PB

The brownish cubic Fe_2O_3 material has been successfully obtained by annealing PB precursor at high temperature.

The IR spectrum of cubic PB precursor in Figure 2 presents its characteristic vibrational bands at 2068 cm^{-1} , 602 cm^{-1} which can be assigned to the vibration of -CN, CN-Fe-CN bonds, respectively.

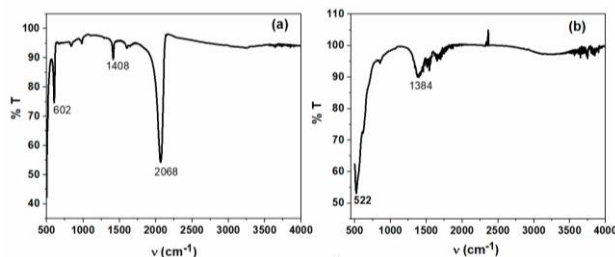


Figure 2. IR spectra of cubic (a) Prussian Blue and (b) cubic Fe_2O_3

The peak at 1408 cm^{-1} can be attributed to the vibration of CH group of remaining PVP [11]. After annealing at 550°C, the organic framework was burnt out, leaving the cubic Fe_2O_3 structure. The strong IR band at 522 cm^{-1} is due to Fe-O vibration [12]. The formation of Fe_2O_3 was also confirmed by Raman spectrum (Figure 3a) in which, peak locates at 498 cm^{-1} is assigned to A_{1g} modes and the five peaks at about 244, 292, 409, and 612 cm^{-1} are attributed to E_g modes [13-14].

XRD pattern of Fe_2O_3 -550 is presented in Figure 3b. The intensive and sharp diffraction peaks at around 24.2°,

33.17°, 35.7°, 40.8°, 49.4°, 54°, 62.47° and 64° can be respectively indexed to the crystal planes of (012), (104), (110), (113), (024), (116), (214) and (300) of hematite α -Fe₂O₃ (JCPDS 33-0664). This implies that the obtained material is pure α -Fe₂O₃. Furthermore, the EDS spectrum obtained on the surface of the material confirmed the existence of Fe and O element with the percentage of 35.68 and 64.32, respectively, roughly describing the elemental ratio of Fe₂O₃ (Figure 3c).

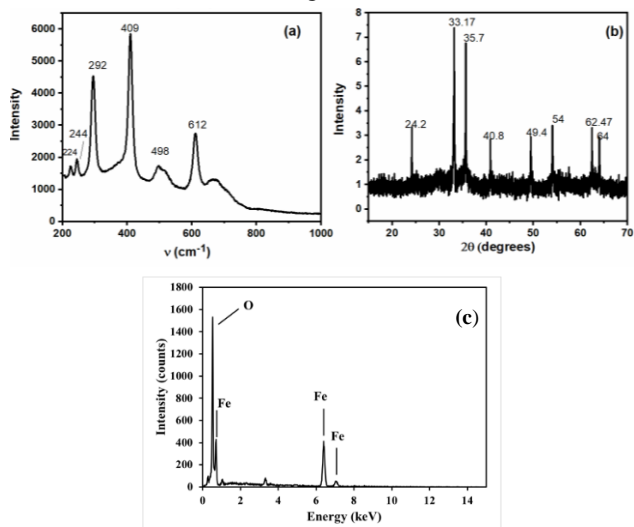


Figure 3. a) Raman spectrum, b) Powder X-ray diffraction and c) EDS spectrum of Fe₂O₃-550

SEM images of Fe₂O₃-550 sample reveal a typical cubic morphology of Fe₂O₃ generated by annealing of PB, with an average size of about 500 nm (Figure 4). However, at an annealing temperature of 650 °C, the aggregation of these particles can be observed.

The tendency to form aggregation at high annealing temperature was also confirmed by the analysis of material surface area. Figure 5 shows the N₂ adsorption-desorption isotherms of Fe₂O₃-550 and Fe₂O₃-650. Specific surface area of Fe₂O₃-550 was calculated to be 30.27 m²/g, while that of Fe₂O₃-650 was 17.45 m²/g. The drop in surface area with an increase of annealing temperature was also reported by Zhang, et al [15], in which annealing of PB at different temperatures leads to the transformation of PB into Fe₂O₃ by the thermally induced oxidative decomposition with different morphology.

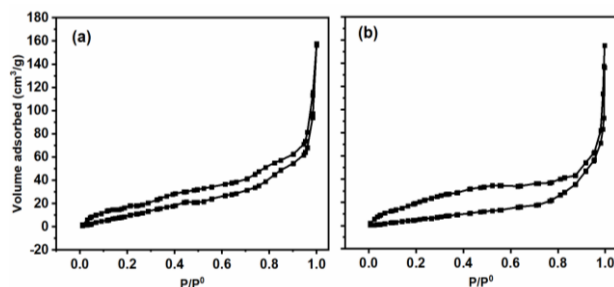


Figure 5. Nitrogen adsorption – desorption isotherms of (a) Fe₂O₃-550 and (b) Fe₂O₃-650 materials

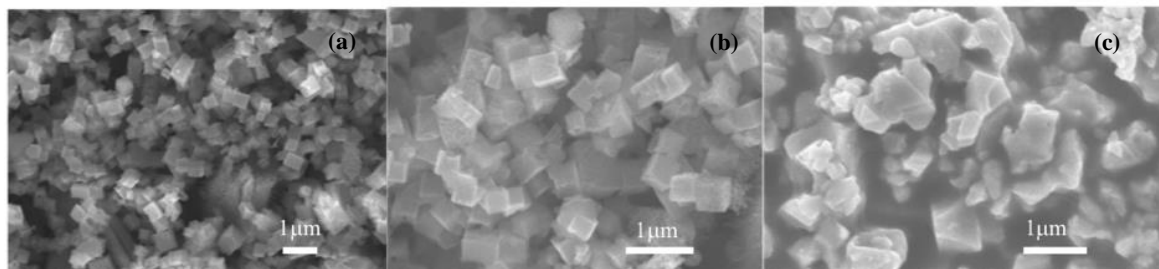
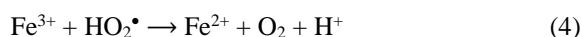


Figure 4. SEM images of Fe₂O₃-550 at 11k (a), 23k magnification (b) and of Fe₂O₃-650 (c)

3.2. Catalytic mechanism

The mechanism of heterogeneous Fenton reaction is widely known with the contribution of free radicals via 2 main stages. H₂O₂ in the solution is firstly activated at the catalyst surface to generate various radical ions which in turn attack the dye molecules in the next stage (Equation 1-5) [4].



To confirm the catalytic role of hydroxyl radical in the degradation of MB in the presence of cubic Fe₂O₃, the degradation efficiency was monitored by adding CH₃OH, which is a OH[•] scavenger, to the reaction mixture at different CH₃OH/H₂O₂ ratio. It is true that the presence of an increased amount of CH₃OH significantly suppresses

the catalytic activity of Fe₂O₃-550. When CH₃OH/H₂O₂ ratio reaches 20:1, this material lost its catalytic activity, which is a strong evidence for the catalytic role of hydroxyl radical (Figure 6).

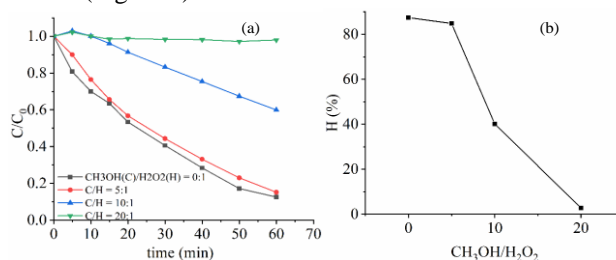


Figure 6. The influence of CH₃OH scavenger on degradation of MB in the presence of Fe₂O₃-550 (C_{MB} = 50 ppm, C_{H₂O₂} = 0.5 M, C_{Fe₂O₃} = 0.3 g/L) a) photocatalytic degradation curves, b) degradation efficiency

3.3. Catalytic activity of microcubes Fe₂O₃

3.3.1. The influence of annealing temperature

In order to investigate the Fenton catalytic behavior of

this material towards MB, the material (0.3 g/L) obtained at various annealing temperatures of 350°C, 550°C and 650°C was dispersed by ultrasonication in an aqueous solution containing MB 50 ppm. H_2O_2 was added to a final concentration of 0.5 M to this mixture after the adsorption equilibrium was reached.

Figure 7a describes the UV-Vis spectra of the solution at different time intervals in the presence of Fe_2O_3 -550. The concentration of MB gradually decreases with the removal efficiency of about 90% after 90 minutes of reaction.

The degradation efficiency was also compared on materials obtained from various annealing temperature. As shown in Figure 7b, when adsorption equilibrium was reached, while Fe_2O_3 -350 and Fe_2O_3 -550 can adsorb about 7% of MB, almost no MB was adsorbed on Fe_2O_3 -650

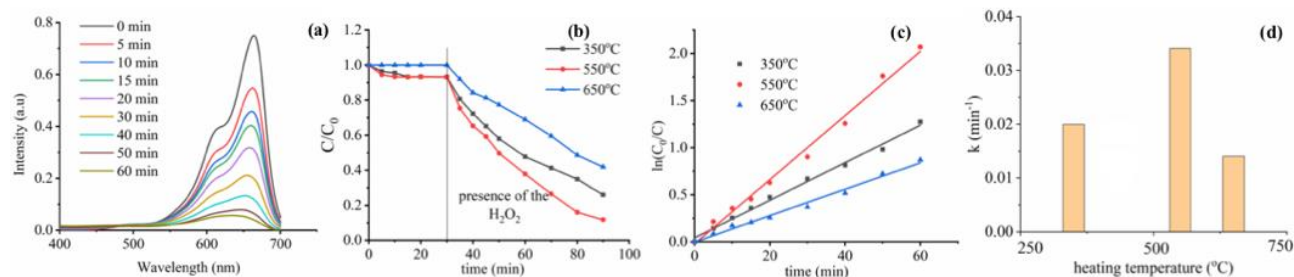


Figure 7. The degradation of MB in the solution containing MB 50 ppm, 0.5 M H_2O_2 , and 0.3 g/L catalyst a) Time dependence UV-Vis spectra of MB in the presence of microcubes Fe_2O_3 -550; b) Relative concentration of MB with time in different oxidation systems; c) The kinetic curves and d) The dependence of rate constant on annealing temperature

3.4. Effects of operational parameters on the degradation of MB

The dependence of degradation efficiency of MB on catalyst dosage was investigated in a mixture containing 50 ppm MB, 0.2 M H_2O_2 with the presence of varied ratio of Fe_2O_3 -550 catalyst from 0 g/L to 0.5 g/L. The kinetics of the reaction is shown in Figure 8.

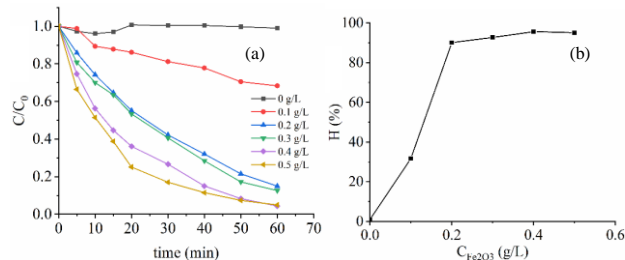


Figure 8. Catalytic degradation kinetics of MB in the presence of different mass ratio of Fe_2O_3 -550, a) degradation curves, b) degradation efficiency ($C_{MB} = 50$ ppm, $C_{H_2O_2} = 0.2$ M)

Increasing the dosage of Fe_2O_3 from 0 g/L to 0.4 g/L significantly enhances the degradation efficiency from 0 to 96 %, as the increase of catalyst dosage provides more active sites which can accelerate the formation of various radical from H_2O_2 . However, the use of 0.5 g/L catalyst leads to a drop in the degradation efficiency which can be attributed to an increase in rate of decomposition of H_2O_2 to O_2 due to thermodynamic and mass transfer limitation [15].

The effect of H_2O_2 concentration is illustrated in Figure 9. It is clear that increasing H_2O_2 concentration from 0 to 0.5 M initially increases the degradation efficiency from 0

material. The poor adsorption capability of Fe_2O_3 -650 is supported by a drop in the BET surface area as described earlier. The dependence of adsorption capability in annealing temperature was also reported by Li. et.al [8].

After the addition of H_2O_2 , all three materials exhibited noticeable catalytic activity with the degradation efficiency of 74%, 88% and 41% for Fe_2O_3 -350, Fe_2O_3 -550, Fe_2O_3 -650 catalyst, respectively. The plot of $\ln C_0/C_t$ vs. time in all three cases is a perfect linear line ($R^2 = 0.99$) implying that the degradation of MB followed a pseudo-first-order kinetics (Figure 7c). The influence of annealing temperature on the rate constant derived from the slope of $\ln C_0/C_t$ vs. time plot is shown in Figure 7d. It is clear that the Fe_2O_3 -550 material exhibits highest catalytic activity in this reaction system with the rate constant of 0.034 min^{-1} . Therefore, Fe_2O_3 -550 was chosen for further investigation.

to 91 %. Nevertheless, further increasing its concentration to 0.7 and 0.9 M does not significantly enhance the degradation efficiency. As aforementioned, the mechanism of this reaction depends mostly on the formation of hydroxyl and peroxide radicals.

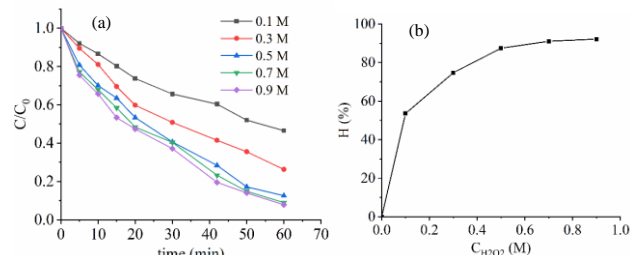


Figure 9. Effect of H_2O_2 concentration on the degradation of MB a) degradation curves, b) degradation efficiency ($C_{MB} = 50$ ppm, $C_{Fe_2O_3} = 0.3$ g/L)

The abundant presence of H_2O_2 in the reaction mixture offers an abundant availability of these radicals leading to the enhancement of degradation efficiency.

However, the excess quantity of H_2O_2 might scavenge hydroxyl radicals by the formation of HO_2^{\cdot} (Eq. 6), which has lower oxidation potential, to form H_2O and O_2 (Eq. 7), interfering with the decomposition of MB [15].



The influence of initial MB concentration of the degradation efficiency was investigated by varying the concentration from 30 to 100 ppm in the presence of 0.5 M

H₂O₂ and 0.3 g/L Fe₂O₃. The degradation efficiency decreases from 96 % to 57% when MB initial concentration increases from 30 ppm to 100 ppm (Figure 10).

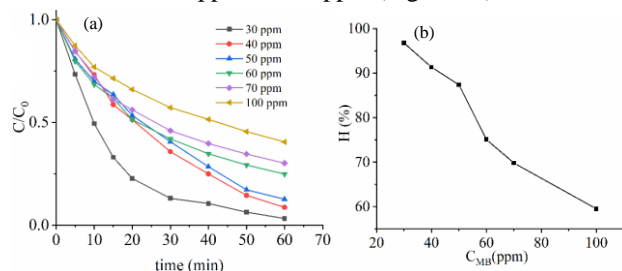


Figure 10. Effect of MB initial concentration on the degradation of MB a) degradation curves, b) degradation efficiency ($C_{H_2O_2} = 0.5 M$, $C_{Fe_2O_3} = 0.3 g/L$)

The adsorption of MB at high concentration might occupy numerous active sites on the catalyst surface hindering the contact of H₂O₂ with the catalyst surface to produce free radical for the degradation reaction. In addition, the intermediates generated in dye degradation process might also compete for the limited adsorption sites with dye molecules, which blocked their interactions with active sites on the catalyst.

Solution pH is known to have significant effect on the catalyst activity as it might alter the catalyst surface. The degradation of MB was also investigated by adjusting solution pH from 3.59 to 9.73 with the addition of the suitable amount of HCl 0.1 M and NaOH 0.1 M.

Figure 11 shows that the highest degradation efficiency of 95 % was obtained at pH = 4.51, nearly double that at pH = 3.59, (H = 54 %). However, further increasing the solution pH leads to a gradual drop in the degradation efficiency.

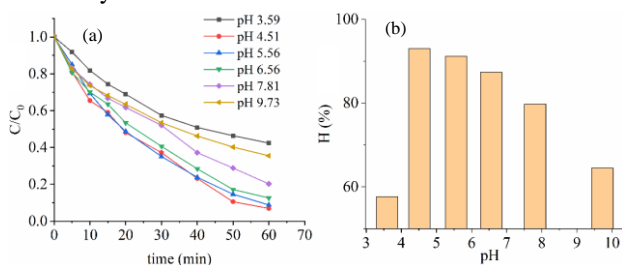


Figure 11. The influence of solution pH on the degradation of MB a) degradation curves, b) degradation efficiency ($C_{MB} = 50 ppm$, $C_{H_2O_2} = 0.5 M$, $C_{Fe_2O_3} = 0.3 g/L$)

In alkaline solution, there is a possibility to form a relatively inactive ferric ion FeO²⁺ (equation 8) or ferric hydroxide complex that can deactivate the catalyst. Furthermore, H₂O₂ can also be decomposed at higher pH, reducing the hydroxyl radical source. In contrast, at low pH, ferrous ions can form iron complex species [Fe(H₂O)₆]²⁺, which hinders the formation of hydroxyl radicals. On the other hand, in the presence of high concentration of H⁺, hydrogen peroxide could be solvated to form stable oxonium ion [H₃O₂]⁺, which also interferes with the production of hydroxyl radicals [15].



The degradation efficiency of this material was compared with its analogue as shown in Table 1. In order

to enhance the catalytic performance in heterogeneous Fenton system, a selection of other oxides or matrixes has been incorporated into Fe₂O₃ structure. For example, Fe₂O₃:SiO₂ composite has shown excellent catalytic capability on MB degradation with the rate constant of 0.113 min⁻¹ [15]. Without any other added metal oxide, pristine cubic Fe₂O₃ in this study exhibits comparable removal efficiency towards MB in heterogeneous Fenton system in comparison with other analogue materials.

Table 1. Comparison on degradation activity of different iron oxide materials

Material	C _{MB} (ppm)	Solid dosage (g/L)	C _{H₂O₂} (M)	k (min ⁻¹)
Fe ₂ O ₃ :SiO ₂ [16]	50	0.5	12 × 10 ⁻³	0.113
Fe ₂ O ₃ /TiO ₂ functionalized biochar [17]	50	0.2	1.45	0.101
Cubic α-Fe ₂ O ₃ (this work)	50	0.3	0.5	0.0398
rGO/Fe ₂ O ₃ /polypyrrole hydrogels [18]	80	0.5	4.8	0.0314
N-doped carbon/CuO-Fe ₂ O ₃ [19]	100	0.5	7.5 × 10 ⁻³	0.0201
α-Fe ₂ O ₃ /SiO ₂ [20]	120	1	1.76 × 10 ⁻³	1.83 × 10 ⁻³
Fe ⁰ -Fe ₃ O ₄ -rGO [21]	50	0.1	0.8 × 10 ⁻³	0.0093
Carbon-doped CuO/Fe ₂ O ₃ [22]	50	0.25	7.5 × 10 ⁻³	6.08 × 10 ⁻³

4. Conclusion

The cubic Fe₂O₃ material has been successfully synthesized by annealing PB precursor. The formation of pure α-Fe₂O₃ was confirmed via spectroscopic results. The cubic morphology of this material was observed in SEM images with the size of around 500 nm. The obtained material had been employed as a heterogeneous catalyst in a Fenton system to degrade MB. With a solution containing 50 ppm MB, 0.5 M H₂O₂ and 0.3 g/L Fe₂O₃, the rate constant of the degradation reaction was determined as 0.0398 min⁻¹ which is comparable with other analogous materials. This result suggests an alternative strategy to synthesis iron oxide materials for the use in organic dyes removal.

Acknowledgements. We would like to acknowledge financial support provided by The Ministry of Education and Training under the grant number B2021-DNA-08.

REFERENCES

- Gupta, V. K.; Suhas; Ali, I.; Saini, V. K., Removal of Rhodamine B, "Fast Green, and Methylene Blue from Wastewater Using Red Mud, an Aluminum Industry Waste", *Industrial & Engineering Chemistry Research*, 43(7), 2004, 1740-1747.
- Bayomie, O. S.; Kandeel, H.; Shoeib, T.; Yang, H.; Youssef, N.; El-Sayed, M. M. H., "Novel approach for effective removal of methylene blue dye from water using fava bean peel waste", *Scientific Reports*, 10 (1), 2020, 7824.
- Mahapatra, K.; Ramteke, D. S.; Paliwal, L. J., "Production of activated carbon from sludge of food processing industry under controlled pyrolysis and its application for methylene blue removal", *Journal of Analytical and Applied Pyrolysis*, 95, 2012, 79-86.
- Zhang, M.-h.; Dong, H.; Zhao, L.; Wang, D.-x.; Meng, D., "A review on Fenton process for organic wastewater treatment based on optimization perspective", *Science of The Total Environment*, 670, 2019, 110-121.

- [5] Yang, X.; Chen, W.; Huang, J.; Zhou, Y.; Zhu, Y.; Li, C., "Rapid degradation of methylene blue in a novel heterogeneous $\text{Fe}_3\text{O}_4@\text{rGO}@\text{TiO}_2$ -catalyzed photo-Fenton system", *Scientific Reports*, 5 (1), 2015, 10632.
- [6] Park, J.-H.; Wang, J. J.; Park, K. H.; Seo, D.-C., "Heterogeneous fenton oxidation of methylene blue with Fe-impregnated biochar catalyst", *Biochar*, 2 (2), 2020, 165-176.
- [7] Tao, Q.; Bi, J.; Huang, X.; Wei, R.; Wang, T.; Zhou, Y.; Hao, H., "Fabrication, application, optimization and working mechanism of Fe_2O_3 and its composites for contaminants elimination from wastewater", *Chemosphere*, 263, 2021.
- [8] Li, X.; Liu, Y.; Zhang, C.; Wen, T.; Zhuang, L.; Wang, X.; Song, G.; Chen, D.; Ai, Y.; Hayat, T.; Wang, X., "Porous Fe_2O_3 microcubes derived from metal organic frameworks for efficient elimination of organic pollutants and heavy metal ions", *Chemical Engineering Journal*, 336, 2018, 241-252.
- [9] Wang, N.; Du, Y.; Ma, W.; Xu, P.; Han, X., "Rational design and synthesis of SnO_2 -encapsulated $\alpha\text{-Fe}_2\text{O}_3$ nanocubes as a robust and stable photo-Fenton catalyst", *Applied Catalysis B: Environmental*, 210, 2017, 23-33.
- [10] Ming, H.; Torad, N. L. K.; Chiang, Y.-D.; Wu, K. C. W.; Yamauchi, Y., "Size- and shape-controlled synthesis of Prussian Blue nanoparticles by a polyvinylpyrrolidone-assisted crystallization process", *CrystEngComm*, 14 (10), 2012, 3387-3396.
- [11] Cheng, Z.; Saad, A.; Adimi, S.; Guo, H.; Liu, S.; Thomas, T.; Yang, M., "Metal organic framework-derived porous Fe_2N nanocubes by rapid-nitridation for efficient photocatalytic hydrogen evolution", *Materials Advances*, 1 (5), 2020, 1161-1167.
- [12] Fardood, S. T.; Ramazani, A.; Golfar, Z.; Joo, S., "Green Synthesis of Fe_2O_3 (hematite) Nanoparticles using Tragacanth Gel", *Quarterly Journal of Applied Chemical Research*, 11, 2017, 19-27.
- [13] Kumar, P.; No-Lee, H.; Kumar, R., "Synthesis of phase pure iron oxide polymorphs thin films and their enhanced magnetic properties", *Journal of Materials Science: Materials in Electronics*, 25 (10), 2014, 4553-4561.
- [14] Mansour, H.; Letifi, H.; Bargougui, R.; De Almeida-Didry, S.; Negulescu, B.; Autret-Lambert, C.; Gadri, A.; Ammar, S., "Structural, optical, magnetic and electrical properties of hematite ($\alpha\text{-Fe}_2\text{O}_3$) nanoparticles synthesized by two methods: polyol and precipitation", *Applied Physics A*, 123 (12), 2017, 787.
- [15] Zhang, L.; Wu, H. B.; Madhavi, S.; Hng, H. H.; Lou, X. W., "Formation of Fe_2O_3 Microboxes with Hierarchical Shell Structures from Metal-Organic Frameworks and Their Lithium Storage Properties", *Journal of the American Chemical Society*, 134 (42), 2012, 17388-17391.
- [16] Vu, A.-T.; Xuan, T. N.; Lee, C.-H., "Preparation of mesoporous $\text{Fe}_2\text{O}_3\text{:SiO}_2$ composite from rice husk as an efficient heterogeneous Fenton-like catalyst for degradation of organic dyes", *Journal of Water Process Engineering*, 28, 2019, 169-180.
- [17] Chen, X.-L.; Li, F.; Chen, H.; Wang, H.; Li, G., " $\text{Fe}_2\text{O}_3/\text{TiO}_2$ functionalized biochar as a heterogeneous catalyst for dyes degradation in water under Fenton processes", *Journal of Environmental Chemical Engineering*, 8 (4), 2020.
- [18] Zhang, J.; Yao, T.; Guan, C.; Zhang, N.; Zhang, H.; Zhang, X.; Wu, J., "One-pot preparation of ternary reduced graphene oxide nanosheets/ Fe_2O_3 /polypyrrole hydrogels as efficient Fenton catalysts", *Journal of Colloid and Interface Science*, 505, 2017, 130-138.
- [19] Ren, B.; Miao, J.; Xu, Y.; Zhai, Z.; Dong, X.; Wang, S.; Zhang, L.; Liu, Z., "A grape-like N-doped carbon/ $\text{CuO-Fe}_2\text{O}_3$ nanocomposite as a highly active heterogeneous Fenton-like catalyst in methylene blue degradation", *Journal of Cleaner Production*, 240, 2019.
- [20] Wu, Z.; Zhu, W.; Zhang, M.; Lin, Y.; Xu, N.; Chen, F.; Wang, D.; Chen, Z., "Adsorption and Synergetic Fenton-like Degradation of Methylene Blue by a Novel Mesoporous $\alpha\text{-Fe}_2\text{O}_3/\text{SiO}_2$ at Neutral pH", *Industrial & Engineering Chemistry Research*, 57(16), 2018, 5539-5549.
- [21] Yang, B.; Tian, Z.; Zhang, L.; Guo, Y.; Yan, S., "Enhanced heterogeneous Fenton degradation of Methylene Blue by nanoscale zero valent iron (nZVI) assembled on magnetic Fe_3O_4 /reduced graphene oxide", *Journal of Water Process Engineering*, 5, 2015, 101-111.
- [22] Ren, B.; Xu, Y.; Zhang, C.; Zhang, L.; Zhao, J.; Liu, Z., "Degradation of methylene blue by a heterogeneous Fenton reaction using an octahedron-like, high-graphitization, carbon-doped Fe_2O_3 catalyst", *Journal of the Taiwan Institute of Chemical Engineers*, 97, 2019, 170-177.